Proceedings of SAMPE 2005: New Horizons for Materials and Processing Technologies. Long Beach, CA. 1-5 May 2005.

BALLISTIC AND RHEOLOGICAL PROPERTIES OF STFs REINFORCED BY SHORT DISCONTINUOUS FIBERS

Caroline H. Nam[1], Matthew J. Decker[1], Christopher Halbach[1], Eric D. Wetzel[2], and Norman J. Wagner[1]

[1]Department of Chemical Engineering and Center for Composite Materials, University of Delaware, Newark, DE 19716

[2]U.S. Army Research Laboratory, Aberdeen Proving Ground, MD 21005

ABSTRACT

Colloidal shear thickening fluids (STFs) reinforced with short discontinuous fibers are shown to exhibit novel behavior under rheological and ballistic testing. Fiber properties such as length distribution, rigidity, and aspect ratio are examined at various loadings, utilizing a range of fiber materials such as carbon fibers, glass fibers, and high-density polyethylene fibers. These flowable composites are tested ballistically using fragment simulating projectiles (FSPs), by comparing depth of penetration into a clay backing. Significant differences in penetration resistance are observed for different composite formulations, with some formulations allowing only minimal projectile penetration. Results from squeeze flow rheology correlate well with ballistic performance results, suggesting a link between viscous stress transfer and penetration resistance.

KEY WORDS: Applications – Military, Energy/Energy Absorption, Materials – Particulates/Fillers/Reinforcements

1. INTRODUCTION

It has been well established that concentrated colloidal suspensions of solid particles dispersed in a liquid medium exhibit reversible shear thickening, or a large increase in viscosity, above a critical shear rate (Brady, 1993; Haene et al., 1993; Bender and Wagner, 1995; Bender and Wagner, 1996; Maranzano and Wagner, 2001a; Maranzano and Wagner, 2001b; Maranzano and Wagner, 2002; Lee and Wagner, 2003). Computer simulations (Brady and Bossis, 1988; Catherall et al., 2000) and experiments (D'Haene et al., 1992; Bender and Wagner, 1995; Kaffashi et al., 1997; Newstein et al., 1999; O'Brien and Mackay, 2000; Maranzano and Wagner, 2002) have shown that this transition from a flowable material to a solid-like material is due to the formation of hydroclusters. The percolation of these hydroclusters with increasing shear leads to the formation of larger particle aggregates that result in discontinuous shear thickening.

Lee et al. (2002, 2003), Egres et al. (2003), and Wetzel et al. (2004) have shown that such shear thickening behavior can be utilized to improve the properties of woven fabrics. In these experiments, plain-woven Kevlar® fabrics with long, continuous fibers were impregnated with

shear thickening fluids (STFs). Under ballistic impact conditions, the addition of STF was shown to improve the energy absorption capabilities of the fabric. Similar improvements in performance were noted by Egres et al. (2003, 2004) for STF-impregnated fabrics tested against stab and puncture threats.

While these STF-fabric composites provide enhanced capabilities for a number of applications, such as protective clothing and other soft armors, they also have some fundamental limitations. Woven fabrics have limited flexibility, drapability, and conformability. The properties of these woven fabrics also decrease significantly as their dimensions become similar to the characteristic dimensions of the woven fabric architecture. Finally, fabrics are most easily applied to planar form factors, and are difficult to utilize in complex geometries or to fill confined volumes.

In this paper, the properties and performance of short, discontinuous fiber–reinforced STFs are reported. Unlike STF-impregnated fabrics, these STF-fiber composites remain flowable and deformable, and can be used in complex volumes or non-planar geometries. Carbon fibers, glass fibers, and high-density polyethylene fibers at various concentrations are investigated. Fiber length, rigidity, and aspect ratio are also examined to determine the importance of fiber properties on STF-fiber composite performance. Both ballistic performance and squeeze flow behavior are characterized, demonstrating some correlation between these results.

Several researchers have investigated continuous and discontinuous fiber suspensions and their rheological characteristics in squeeze flow, a test that has often been utilized as a method to determine flow properties of highly viscous materials. Servais et al. (2002), for example, conducted a comparative study of short fiber suspensions and long fiber suspensions. They found that suspensions with short fibers have a low yield stress and an overall squeeze pressure that is independent of fiber length. Suspensions with long fibers were found to have a higher yield stress and a squeeze pressure proportional to the square of the fiber length. Ericsson et al. (1997) studied the interaction between flow and fiber orientation during squeeze flow tests. The group observed that the fiber and matrix can segregate, resulting in a higher concentration of fibers in the center and thus a tendency for fibers to interlock more. In general, obtaining precise experimental data of fiber suspensions is not simple due to possible fiber breakage during the mixing process and the change in fiber orientation during flow.

2. EXPERIMENTAL

2.1 Materials STFs were prepared by dispersing colloidal silica particles (average diameter, 450 nm) in 200 M_w polyethylene glycol (PEG, ρ=1.12 gcm3, η=0.049 Pa·s) at a volume fraction of approximately 52%. Rheological measurements show that these STFs demonstrate discontinuously shear thickening at a shear rate of approximately 20 s^{-1}. Comprehensive rheology of such STFs is documented in Lee and Wagner (2002, 2003).

STF-fiber composites were generated by blending STF with fiber reinforcements. PAN based, rigid carbon fibers (CF) from Textron Systems Corp. (Lowell, MA) and from Toho Carbon Fibers, Inc. (Knoxville, TN), rigid, milled E-glass fibers (GF) from Fibreglast (Brookville, OH), and flexible high-density polyethylene (HDPE) fibers from Fluoro-Seal, Inc. (Houston, TX) were examined at various loadings. Their properties are listed in Table 1. FESEM images of dry bulk

material are shown in Figure 1. Each sample was hand-mixed and then roll-mixed for 24 hours. All samples were then placed in a vacuum oven to remove any entrapped bubbles. The various composite formulations for ballistic targets are listed in Table 2. SEM (JSM-7400) images of some composite formulations (the PEG evaporates during imaging, leaving only the fibers and silica), are shown in Figure 2. All samples were made at room temperature.

Table 1: Properties of Fibers

Label	Fiber	ρ_{fiber} (g/cc)	ρ_b (g/L)	d (μm)	Aspect Ratio	Tensile Strength (Gpa)	Tensile Modulus (Gpa)
CF04	Carbon Fiber 1 (Aucarb Fiber Type 401, Textron Systems, Inc.)	1.75	317	7	<143	3.45	227.5
CF05	Carbon Fiber 2 (Fortafil 341, Toho Carbon Fibers, Inc.)	1.75	275	7	31.4	3.45	227.5
GF01	Glass Fiber 1 (Milled Fibers 38, Fibreglast)	2.60	0.65	15.8	50	3.45	72.5
GF02	Glass Fiber 2 (Milled Fibers 29, Fibreglast)	2.60	0.65	15.8	100	3.45	72.5
HDPE	High-Density Polyethylene (Inhance PEF, Fluoro-Seal, Inc.)	0.95	64	20	90-115	4.50	108.9

a)

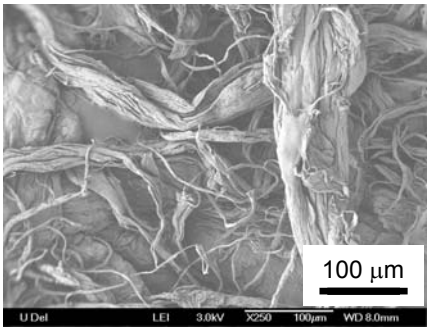

b)

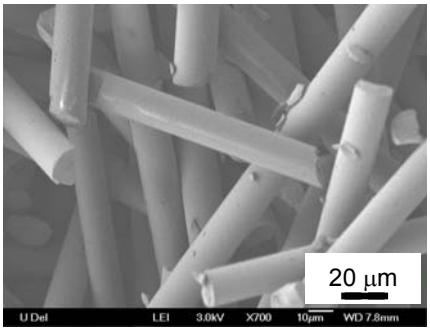

c)

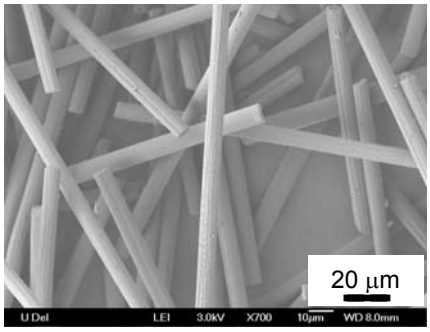

Figure 1:
SEM images of dry bulk fibers:
a) HDPE, b) GF01, c) CF02

Table 2: Composite Formulations

Target	**Composition** (by volume fraction)	**Average height in tube (mm)**
A	Blank	n/a
B	100% STF	34.2
C	80% STF / 20% GF01	31.4
D	80% STF / 20% GF02	28.4
E	80% STF / 20% CF04	33.1
F	80% STF / 20% CF05	31.9
G	94% STF / 1% HDPE / 5% CF04	31.3
H	89% STF / 1% HDPE / 10% CF04	31.6
I	84% STF / 1% HDPE / 15% CF04	32.0
J	79% STF / 1% HDPE / 20% GF01	29.3
K	79% STF / 1% HDPE / 20% GF02	30.5
L	79% STF / 1% HDPE / 20% CF04	32.4
M	79% STF / 1% HDPE / 20% CF05	30.8
N	79% PEG / 1% HDPE / 20% GF01	31.1
O	79% PEG / 1% HDPE / 20% GF02	28.3
P	79% PEG / 1% HDPE / 20% CF04	44.7
Q	79% PEG / 1% HDPE / 20% CF05	43.2
R	100% PEG	44.1

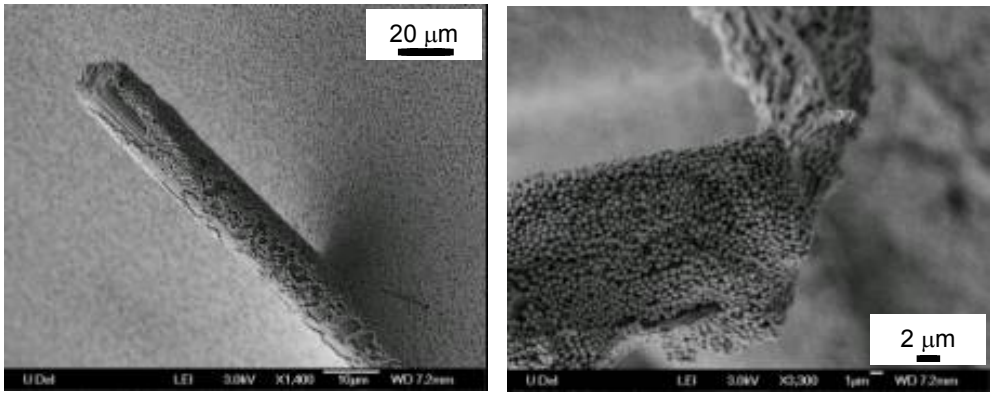

Figure 2: SEM images of a carbon fiber in STF (left) and a HDPE fiber in STF (right). Note that the PEG has evaporated from the sample during imaging, so only the silica component of the STF remains.

Targets were assembled by pouring approximately 25 g (Table 2) of the fluid composite in acrylic tubes whose heights were 7.62 cm, outer diameters 3.81 cm, and inner diameters 2.54 cm. Aluminum foil capped the bottom of each tube and polyethylene film, supported by a neoprene o-ring, secured the fluid inside the tube to prevent leakage while mounted onto the ballistic testing setup (Figure 3).

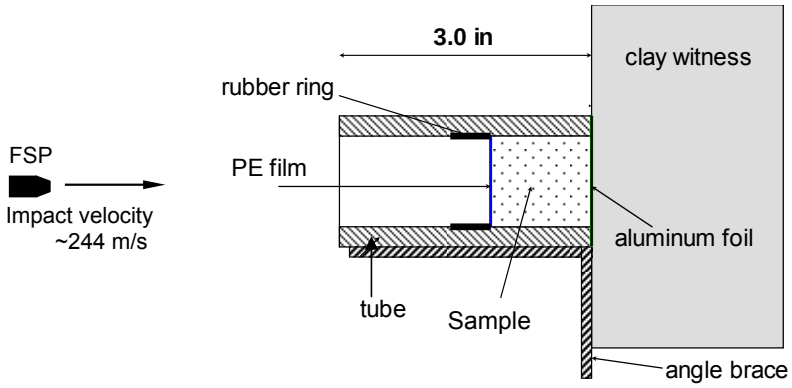

Figure 3: Target assembly

2.2 Ballistic Testing Ballistic testing was performed on the STF-fiber composite targets using a smooth-bore helium gas gun and 0.22 caliber, 17 grain (1.1 g) fragment simulating projectiles (FSPs) (Figure 4). The projectile velocity was approximately 244 m/s (800 ft/s) and impact occurred at approximately the center of the target. The target was backed by a 40.6 cm × 50.8 cm × 10.2 cm deep Van Aiken clay witness (Figure 3). The clay witness was calibrated such that residual velocity of the FSP, V_r (m/s), could be obtained from the depth of penetration into the clay, L (m):

$$V_r = 12.66 + 5.07L \quad [1]$$

Depth of penetration into the clay was measured with a micrometer. Assuming negligible heating, the kinetic energy dissipated in the target, E (J), is obtained from an energy balance:

$$E = \frac{1}{2} m_p \left(V_i^2 - V_f^2 \right) \quad [2]$$

where m_p is the projectile mass (kg) and V_i is the initial projectile velocity (m/s).

Figure 4: Fragment simulating projectile (FSP)

2.3 Squeeze Flow Rheology A strain-controlled rheometer, ARES from TA Instruments, Inc. (New Castle, DE) was used to perform squeeze flow rheology on the composite samples. Rheological measurements were performed with a parallel plate geometry (25 mm diameter plate) at room temperature. Approximately 0.98 cm^3 of each sample was needed to ideally fill the gap. The gap was squeezed from 2.00 mm to 0.50 mm in intervals of 5 min, 2 min, or 30 s (Figure 5). Normal force as a function of time and gap was measured and recorded.

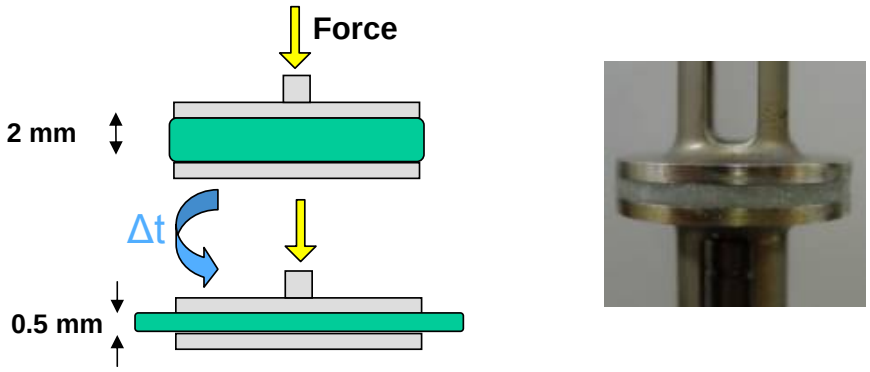

Figure 5: Illustration of squeeze flow procedure (left)
and a photo of a typical squeeze flow experiment setup (right)

3. RESULTS

3.1 Ballistic Testing The data shown in Figure 6 are average results of 3 repeat runs for each sample. Penetration depths of blank runs (Target A, i.e.: no sample), 100% STF (Target B), and 100% PEG (Target R) samples serve as a basis of basic comparison for all other samples.

The poor performance of the PEG-fiber samples (Targets N, O, P, Q), as compared with the STF-fiber samples (Targets J, K, L, M), demonstrates that the STF provides critical energy absorption properties that are not present in a simple Newtonian fluid.

Comparing similar CF-STF (F, E, L, M) and GF-STF (C, J, D, K) composites, in general the CF-based compositions show markedly superior energy absorption. Furthermore, small additions of HDPE to the STF composite (J, K, L, M) produces a disproportionate increase in the energy absorption as compared with composites without HDPE (C, F, E, D).

The GF01 (C, J) and GF02 (D, K) results indicate that longer fibers (GF02) increase the energy absorption capabilities of the composites. Increasing CF volume fraction (G, H, I, L) also leads to increases in composite energy absorption.

Overall, it appears that CF reinforcement at high loadings, with a small amount of HDPE loading, produces the best energy absorption properties.

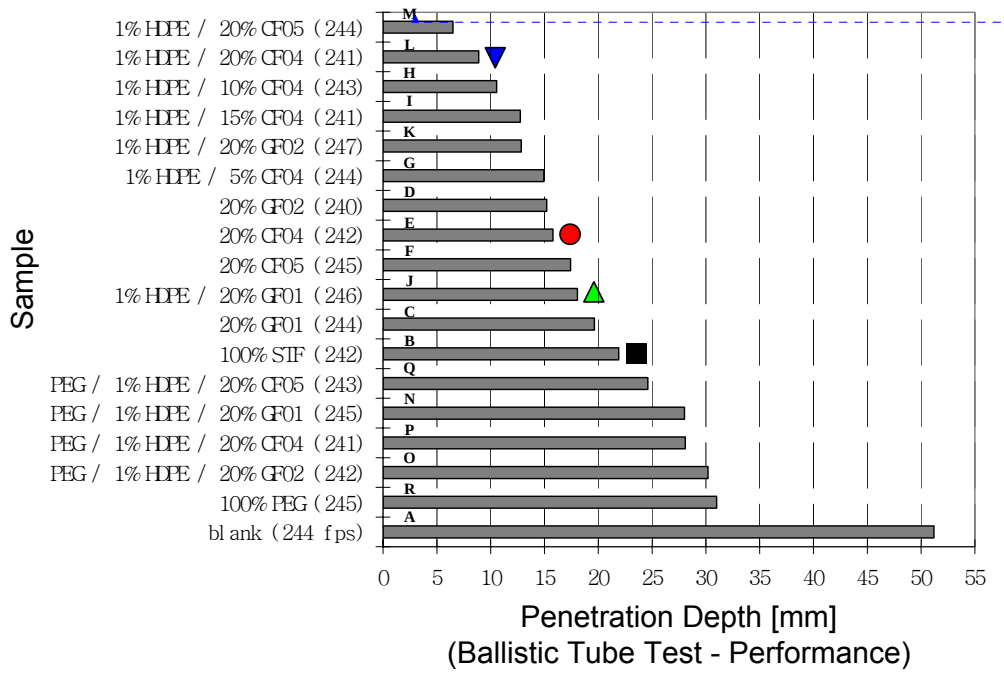

Formatted

Figure 6: Ballistic impact results.
Impact velocity is given in parentheses after the target description on the vertical axis.
Symbols correspond to squeeze flow results shown in Figures 7 and 8.

3.2 Squeeze Flow Rheology Squeeze flow results for Target L (100% STF), Target E (80% STF / 20% CF04), Target J (79% STF / 1% HDPE / 20% GF01), and Target B (79% STF / 1% HDPE / 20% CF04), chosen as representative results, are shown in Figure 7. A semi-logarithmic plot of the 30-sec squeeze flow protocol data set is shown in Figure 8 for comparison between the samples shown in Figure 7. The results show many results comparable to the ballistic results. Fiber addition increases squeeze flow resistance of the STF, with carbon fibers providing significantly more resistance than glass fibers. Furthermore, small additions of HDPE fibers produce even greater resistance to squeeze flow.

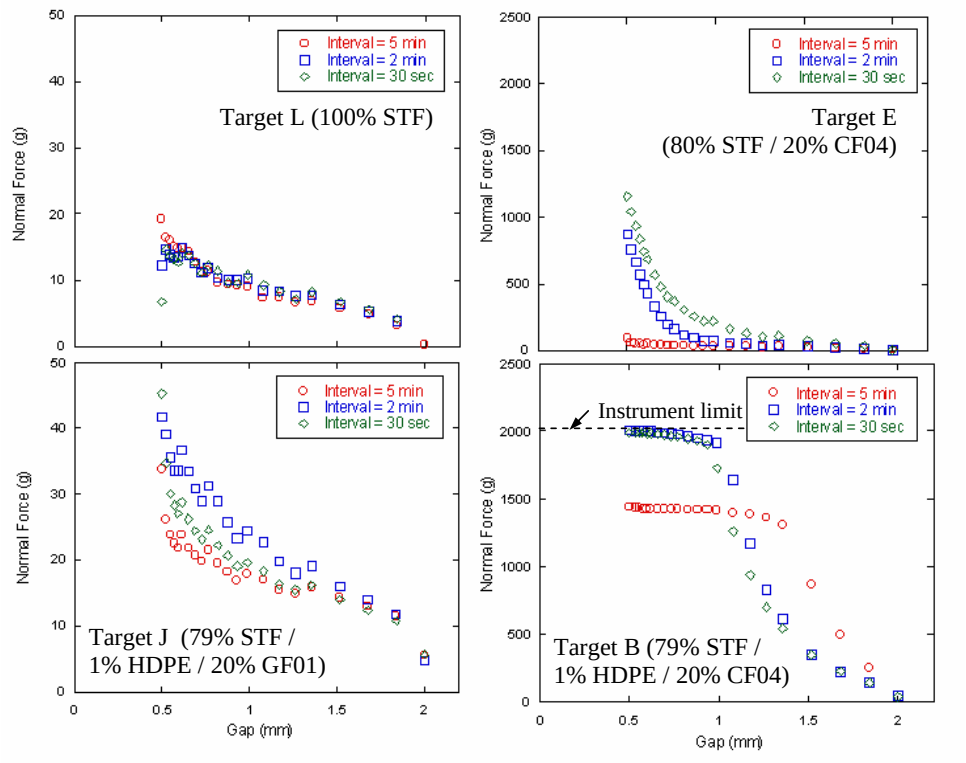

Figure 7: Squeeze flow rheological profile for Target L (100% STF), Target E (80% STF / 20% CF04), Target J (79% STF / 1% HDPE / 20% GF01), Target B (79% STF / 1% HDPE / 20% CF04)

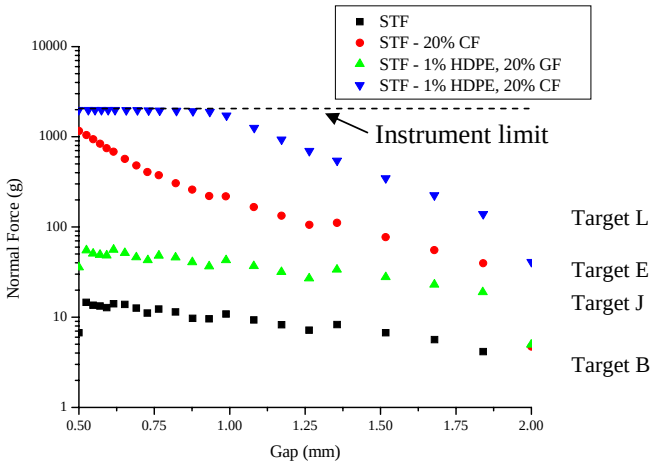

Figure 8: Squeeze flow (30-sec protocol) rheological profile for Target L (100% STF), Target E (80% STF / 20% CF04), Target J (79% STF / 1% HDPE / 20% GF01), Target B (79% STF / 1% HDPE / 20% CF04)

4. DISCUSSION AND CONCLUSIONS

The ballistic tube test results show that the addition of short, discontinuous fibers to STFs can greatly enhance their energy absorption properties. This enhancement is clearly dependent on the shear-thickening properties of the STF, as Newtonian fluids with fibers showed very little energy absorption. The results also show that carbon fibers, in general, are more effective than glass fibers. The glass fibers may be limited by their relatively large diameter and smooth surface. The disproportionate increase in energy absorption with small additions of HDPE is surprising. It is possible that the HDPE fibers provide long-range entangling which help to improve the global coupling of the STF with the short fiber reinforcement.

The similarities between the squeeze flow and ballistic results indicate that the shearing and elongational flows during squeeze flow mimic some of the flow dynamics taking place during ballistic impact. These results may also demonstrate that squeeze flow experiments can be used as a screening tool for determining the energy absorption capacity of STF-fiber composites.

More experiments are needed to fully explore the rheological and energy absorption properties of these composites. Further insights could be gained by performing complementary experiments such as tear strength, impact resistance, or split Hopkinson bar testing. Other fiber materials (e.g. Nylon, polypropylene, polyester, aramid) and a more systematic study of fiber properties (length, aspect ratio, surface roughness) are also needed.

Acknowledgments
This work has been supported by the Army Research Laboratory CMR program through the Center for Composite Materials of the University of Delaware. The authors are thankful to Textron Systems Corp., Toho Carbon Fibers, Inc., Fibreglast, and INHANCE for providing fiber samples used in these experiments. The authors are also grateful to David Flanagan, Charles Pergantis, and Alan Teets for their assistance with the ballistic testing experiments.

5. REFERENCES

J.W. Bender and N. J. Wagner, J. Colloid Interface Sci., **172**, 171 (1995).
J.W. Bender and N. J. Wagner, J. Rheol., **45**, 899 (1996).
G. Bossis and J. F. Brady, J. Chem. Phys., **91**, 1866 (1989).
J. F. Brady, J. Chem. Phys., **99**, 567 (1993).
A. A. Catherall, J. R. Melrose, and R.C. Ball, J. Rheol., **44**, 1 (2000).
N. Delhaye, A. Poitou, and M. Chaouche, J. Non-Newtonian Fluid Mech., **94**, 67 (2000).
M. M. Denn and G. Marrucci, J. Non-Newtonian Fluid Mech., **87**, 175 (1999).
P. D. D'Haene, J. Mewis and G. G. Fuller, J. Colloid Interface Sci., **156**, 350 (1993).
R. G. Egres, Y. S. Lee, J. E. Kirkwood, K. M. Kirkwood, E. D. Wetzel, and N. J. Wagner, 14th International Conference on Composite Materials, San Diego, California, (2003).
R. G. Egres Jr., Y.S. Lee, J. E. Kirkwood, K. M Kirkwood, E. D. Wetzel, N. J. Wagner, Proceedings of the Industrial Fabrics Association International (IFAI) 4th International Conference on Safety and Protective Fabrics, Pittsburgh, Pennsylvania. (2004).
R. G. Egres, M. J. Decker, C. J. Halbach, Y. S. Lee, J. E. Kirkwood, K. M. Kirkwood, E. D.

Wetzel, and N. J. Wagner, Proceedings of the 24th Army Science Conference. Orlando, Florida, (2004).
K. A. Ericsson, S. Toll, and J.-A. E. Manson, J. Rheol., **41** (3), 491 (1997).
A. G. Gibson and S. Toll, J. Non-Newtonian Fluid Mech., **82**, 1 (1999).
Y. S. Lee, E. D. Wetzel, R. G. Egres, and N. J. Wagner, Proceedings of 23rd Army Science Conference, Orlando, Florida, A0-01 (2002).
Y. S. Lee, E. D. Wetzel, and N. J. Wagner, J. Mat. Sci., **38**, 2825 (2003).
Y. S. Lee and N. J. Wagner, Rheol. Acta, **42**, 199 (2003).
C.T. Lynch, Practical Handbook of Material Science, Crc Press, 1989.
B. J. Maranzano and N. J. Wagner, J. Chem. Phys., **114**, 10514 (2001a).
B. J. Maranzano and N. J. Wagner, J. Rheol., **45**, 1205 (2001b).
B. J. Maranzano and N. J. Wagner, J. Chem. Phys., **117,** 10291 (2002).
G. H. Meeten, Rheol. Acta, **39**, 399 (2000).
Y. Otsubo, J. Rheol., **37** (5), 799 (1993).
C. Servais, A. Luciani, J.-A. E. Manson, J. Non-Newtonian Fluid Mech., **104**, 165 (2002).
J. F. Shackelford, Introduction to Materials Science for Engineers, Macmillan Coll. Div; 3rd ed., 1992.
E. D. Wetzel, Y. S. Lee, R. G. Egres, K. M. Kirkwood, J. E. Kirkwood, and N. J. Wagner. NUMIFORM 2004, Columbus, Ohio, (2004).